

**STRUCTURAL CHANGES, EXPRESSION OF
DREAM, BDNF AND CREB PROTEINS IN THE
HIPPOCAMPUS; AND SPATIAL LEARNING AND
MEMORY OF RAPID EYE MOVEMENT (REM)
SLEEP-DEPRIVED RATS UPON ACUTE
NICOTINE TREATMENT**

NORLINDA BINTI ABD RASHID

UNIVERSITI SAINS MALAYSIA

2018

**STRUCTURAL CHANGES, EXPRESSION OF
DREAM, BDNF AND CREB PROTEINS IN THE
HIPPOCAMPUS; AND SPATIAL LEARNING AND
MEMORY OF RAPID EYE MOVEMENT (REM)
SLEEP-DEPRIVED RATS UPON ACUTE
NICOTINE TREATMENT**

by

NORLINDA BINTI ABD RASHID

Thesis submitted in fulfillment of the requirements

for the degree of

Doctor of Philosophy

July 2018

ACKNOWLEDGEMENTS

Alhamdulillah, in the name of Allah, the Most Beneficent and the Most Merciful

I am deeply thankful to my dear main supervisor, Dr Idris Long, and co-supervisors Prof. Dr. Zalina Ismail, Dr. Hermizi Hapidin and Assoc. Prof. Dr. Hasmah Abdullah, for guidance, support, patience and giving me a golden opportunity to start and complete this study.

I would also like to express my gratitude to the Director of BRAINetwork Centre for Neurocognitive Science, Head of Department and staff of ARASC and the Central Research Lab USM Kubang Kerian for giving me the opportunity to work in their laboratories. A special thanks is extended to the Manager and laboratory staff of the Electron Microscopy Unit, University Malaya for their assistance and support.

To my parents, and husband Saberi Bin Dick, thanks for being my backbone and for giving me the support and strength to complete this study.

Finally, I would like to acknowledge Universiti Sains Malaysia for the financial support Short Term Grant [304/PPSK/61312093], P3NEURO Grant [304/PPSK/652204/K134], Research University Grant [1001/PSK/8630023] and Fundamental Research Grant Scheme [203/PPSK/6171153], that were provided for completion of this study.

TABLE OF CONTENTS

Acknowledgements	ii
Table of Contents	iii
List of Table	xi
List of Figures	xii
List of Appendices	xxiii
List of Abbreviations	xxiv
Abstrak	xxxix
Abstract	xxxiii
CHAPTER 1 - INTRODUCTION	1
1.1 Sleep	1
1.1.1 History of sleep study	2
1.1.2 Sleep process	3
1.1.2(a) Waking state	4
1.1.2(b) Wake-promoting system	6
1.1.2(c) Sleep initiation	6
1.1.3 Sleep categories	9
1.1.3(a) NREM sleep phase	9
1.1.3(b) REM sleep phase	10
1.1.3 (c) Mechanism of REM sleep generation	14
1.1.3 (d) REM sleep maintenance	14
1.2 REM Sleep Deprivation	15

1.2.1	REM sleep deprivation (REMsD) models	16
1.2.2	Effect of REMsD on the animal behaviour	19
1.2.3	Effect of REMsD on the neuronal morphology	21
1.2.4	Effect of REMsD on the learning and memory	22
1.3	Learning and Memory	22
1.3.1	Learning in animal	23
1.3.2	Mechanism of learning process	25
1.3.3	Mechanism of memory process	26
	1.3.3(a) Implicit memory	27
	1.3.3(b) Explicit memory	29
	1.3.3(c) LTP in the mossy fibres pathway	30
	1.3.3(d) LTP in the Schaffer collateral and perforant pathways	33
1.3.4	Learning and memory assesment	37
	1.3.4(a) Morris Water Maze paradigm	37
	1.3.4 (b) Probe test of Morris Water Maze	39
	1.3.4(c) MWM test and the function of hippocampus	40
1.4	Hippocampus	41
	1.4.1 Anatomy and the role of the hippocampus	41
1.5	Nicotine	45
	1.5.1 History, structure and metabolites of nicotine	45
	1.5.2 Therapeutic use of nicotine	48
	1.5.3 Effects of nicotine on the hippocampal receptors	49
	1.5.4 Nicotine and cognitive function	51

1.5.5	Nicotine and REMsd induced learning and memory impairment	52
1.6	Downstream Regulatory Element Antagonistic Modulator (DREAM) Protein	54
1.6.1	The structure of DREAM protein	56
1.6.2	The role of DREAM protein	56
1.6.3	The role of DREAM protein in learning and memory	59
1.7	Cyclic Amp Response Element-Binding Protein (CREB)	60
1.7.1	CREB protein and CREB binding protein (CBP)	60
1.7.2	The structure of CREB protein	61
1.7.3	The role of CREB protein	64
1.7.4	The role of CREB protein on learning and memory	66
1.8	Brain Derived Neurotrophin Factor (BDNF)	68
1.8.1	The identification of BDNF protein	68
1.8.2	The role of BDNF protein	69
1.8.3	The structure of BDNF protein	70
1.8.4	The role of BDNF protein on learning and memory	73
1.9	Structural changes during REMsd	75
1.10	Rationale And Aims Of The Study	77
1.11	Objectives Of The Study	79
1.12	Study Hypotheses	80
	CHAPTER 2 - MATERIALS AND METHODS	81
2.1	Materials	81
2.2	Animal	81

2.2.1	Acclimatisation	86
2.2.2	Induction of REM sleep deprivation	86
2.3	Nicotine Treatment	90
2.4	Measurement of Blood Cotinine	90
2.4.1	Blood sample collection via cardiac puncture	90
2.4.2	Serum preparation	91
2.4.3	Measurement of blood cotinine using ELISA	91
2.5	Food Consumption and Body Weight Gain Assessment	96
2.6	Spatial Learning and Memory Performance Measurement by Morris Water Maze Test	97
2.7	Immunohistochemistry Analysis	100
2.7.1	Sacrifice of the animals and perfusion-fixation of the brain	100
2.7.2	Cryostat sectioning	102
2.7.3	DREAM, pCREB and BDNF protein immunopositive slides preparation	102
2.7.4	Counting of DREAM or pCREB or BDNF positive neurons	104
2.8	Western Blot Analysis	107
2.8.1	Protein extraction	107
2.8.2	Protein concentration measurement	108
2.8.3	Sodium Dodecyl Sulphate Polyacrylamide gel (SDS-PAGE) electrophoresis	110
2.8.4	Preparation of resolving gel (12%)	110
2.8.5	Preparation of stacking gel (4%)	111

2.8.6	Electrophoresis of SDS-PAGE gel	112
2.8.7	Electrophoretic transfer and immunoblotting	112
2.8.8	Measurement of mean relative intensity (fold changes)	117
2.9	Transmission Electron Microscopy (TEM) Analysis	118
2.9.1	Primary fixation and post fixation	118
2.9.2	Dehydration	118
2.9.3	Preparation of resin mixture	119
2.9.4	Infiltration, embedding and polymerization	119
2.9.5	Glass knives preparation	119
2.9.6	Thick or semi-thin sectioning	120
2.9.7	Ultrathin sectioning	121
2.9.8	Staining for TEM	121
2.9.9	Semi quantitative histology examination	126
2.10	Statistical Analysis	133
	CHAPTER 3 - RESULTS	134
3.1	Effects of Rem Sleep Deprivation On Food Consumption and Body Weight Gain	134
3.1.1	Food consumption (Fc)	134
3.1.2	Body weight gain (BWg)	138
3.2	Serum Blood Cotinine Level	142
3.3	Spatial Learning and Memory Performance Measurement by Morris Water Maze Test	144
3.3.1	Escape latency (EL) time	144

3.3.2	Distance travelled (DT)	148
3.4	Swimming Speed (SS)	152
3.5	Probe Test on the 6 th Day of MWM Test	156
3.6	Immunohistochemical Analysis	159
3.6.1	DREAM protein expression	162
3.6.2	pCREB protein expression	170
3.6.3	BDNF protein expression	179
3.7	Western Blot	188
3.7.1	Mean relative DREAM protein level in the hippocampus	188
3.7.2	Mean relative total CREB and phosphorylated/total protein level in the hippocampus	190
3.7.3	Mean relative BDNF protein level in the hippocampus	193
3.8	Transmission Electron Microscopy (TEM)	195
3.8.1	Ultrastructure scores for the CA1 region of the hippocampus	195
3.8.2	Ultrastructure scores for the CA2 region of the hippocampus	202
3.8.3	Ultrastructure scores for the CA3 region of the hippocampus	208
3.8.4	Ultrastructure scores for the DG region of the hippocampus	214
CHAPTER 4 - DISCUSSION		220
4.1	Assessment of REMsd	221
4.1.1	Increased Fc but decreased the body weight in REMsd	221
4.2	Subcutaneous Administration of Nicotine	225
4.2.1	Serum blood cotinine	225
4.3	Effects of REMsd and Acute Nicotine Treatment On Spatial Learning	

And Memory Performance Based On MWM Test	229
4.3.1 Effects of REMsd and acute nicotine treatment on escape latency (EL)	230
4.3.2 Effects of REMsd and acute nicotine treatment on distance travelled (DT)	234
4.3.3 Effects of REMsd and acute nicotine treatment on swimming speed (SS)	236
4.3.4 Effects of REMsd and acute nicotine treatment on percentage of time spent in target quadrant in probe test	238
4.3.5 Effect of REMsd and acute nicotine treatment on swimming pattern during probe test	240
4.4 Effects of REMsd On DREAM, CREB, and BDNF Protein Expression	241
4.4.1 Effect of REMsd on DREAM protein expression	242
4.4.1(a) Effects of REMsd and acute nicotine treatment on DREAM-positive neurons (DPN)	242
4.4.1(b) Effect of REMsd and acute nicotine treatment on mean number of DPN in hippocampus	244
4.4.1(c) Effect of REMsd and acute nicotine treatment on mean relative DREAM protein levels in hippocampus	247
4.4.2 Effects of REMsd on CREB and BDNF protein expression	249
4.4.2(a) Effects of REMsd acute nicotine treatment on pCPN and BPN proteins	251
4.4.2(b) Effects of REMsd and acute nicotine treatment on the	

mean number of pCPN and BPN in hippocampus	254
4.4.2(c) Effects of REMsd and acute nicotine treatment on the mean relative phosphorylated CREB/ total CREB ratio and BDNF protein levels in the hippocampus	255
4.5 Effects of REMsd and Acute Nicotine Treatment On Ultrastructure of Hippocampal Neurons	257
4.5.1 Effects of REMsd on hippocampal neuron ultrastructures	257
4.5.2 Effects of REMsd and acute nicotine treatment on the ultrastructures of hippocampal neurons	260
4.6 Overall Findings From the Study	262
CHAPTER 5 – SUMMARY AND CONCLUSION	262
5.1 Summary and Conclusion	263
5.2 Limitations and Further Directions	268
REFERENCES	270
APPENDICES	
LIST OF PUBLICATIONS AND PRESENTATIONS	

LIST OF TABLE

	Page
Table 2.1 Ultrastructure scoring system	128

LIST OF FIGURES

		Page
Figure 1.1	Waking and sleep stages.	5
Figure 1.2	A schematic drawing showing key components of the ascending arousal system. The groups of neurons that are responsible to the wake-promoting system located in LC (locus coeruleus), RN (raphe nuclei), PPT (pedunculo pontine tegmentum), SNc (substantia nigra compacta) and VTA (ventral tegmental area).	8
Figure 1.3	The expression of REM sleep using Cellular-Molecular-Network (CMN) model on the activity of cholinergic and aminergic system.	13
Figure 1.4	Hippocampal trisynaptic loop consists of perforant pathway (input connection from entorhinal cortex (EC) axons synapse into granule cells of dentate gyrus (DG)), mossy fibre pathway (axons from granule cells of DG synapse into the CA3 pyramidal neurons), and Schaffer Collateral pathway (axons from CA3 cells synapse into the CA1 cells), the loop is completed when CA1 axons projected to the EC.	32
Figure 1.5	Schematic diagram showing the formation of early and late LTP.	36

Figure 1.6	Morphology of hippocampal principal cells (neuron). Pyramidal cells of the CA1, CA2, and CA3 region (A). Three-dimensional structure of a CA1 pyramidal cell illustrated from frontal, side, and top views (B). Morphological diversity of DG GCs (C). Values adjacent to the cells indicate the total dendritic length. Note the difference between the upper (supra- pyramidal) and lower (infra-pyramidal) blades. Three-dimensional structure of a GC illustrated from frontal, side, and top views (D).	44
Figure 1.7	The nicotine chemical empirical formular (C_5H_7N) that was described by Melsens in 1843.	48
Figure 1.8	Ribbon representation of DREAM protein structure consisting of nonconserved N-terminal region and four EF-hand, determined by Nuclear Magnetic Resonance (NMR) spectroscopy.	58
Figure 1.9	Ribbon representation CREB protein structure (blue) with phosphorylated Ser 133 (green) and interaction with KIX domain of CBP (red).	63
Figure 1.10	The route of BDNF protein from synthesis to secretion.	71
Figure 1.11	The structure of BDNF protein. Different views showing the main structure of the heterodimer (A),	

	and its main secondary conformations (β -strands)	
	(B). Neurotrophin structure homology showing mouse NGF (light blue), and human BDNF (red), NT3 (yellow) and NT4 (dark blue) in the same orientation (C).	72
Figure 2.1	Number of animals used for the study.	83
Figure 2.2	Flow chart of experimental design.	85
Figure 2.3	Acclimatisation phase.	88
Figure 2.4	REM sleep deprivation phase.	89
Figure 2.5	Procedure of blood cotinine measurement using ELISA.	93
Figure 2.6	Serum cotinine standard concentration graph.	95
Figure 2.7	Illustration of Morris Water Maze paradigm.	99
Figure 2.8	Perfusion fixation technique.	101
Figure 2.9	Flow chart of immunohistochemistry analysis.	105
Figure 2.10	Hippocampus tissue showing the regions of connus ammonis (CA) and dentate gyrus (DG).	106
Figure 2.11	Flow chart of hippocampus protein extraction protocol	109
Figure 2.12	Protocol for Western Blot analysis.	116
Figure 2.13	Glass knives preparation using Leica Reichert Knifemaker, Austria (A); the glass strips were placed on the strip holding plate before they were cut (B);	

	first the glass strip was cut into square, then the square glass was cut into triangle, forming a glass knife (C).	122
Figure 2.14	Sample resin block trimming using Gillette Super Nacet blade (A), trapezium shaped trimmed resin block (B) and semi-thin sectioning using glass knife (C).	123
Figure 2.15	Ultrathin sectioning using diamond knife (A), ultrathin section transferred on the copper grid (Mesh 300) (B) and copper grids containing ultrathin sections (C).	124
Figure 2.16	Flow chart of transmission electron microscopy (TEM) analysis.	125
Figure 2.17	Image for cytoplasm assessment score of transmission electron microscopy.	129
Figure 2.18	Image for nucleus assessment score of transmission electron microscopy.	130
Figure 2.19	Image for mitochondria assessment score of transmission electron microscopy.	131
Figure 2.20	Image for rough endoplasmic reticulum (RER) assessment score of transmission electron microscopy.	132
Figure 3.1	Food consumption (g/day per kg ^{0.67}) during the	

	period of adaptation for all groups.	135
Figure 3.1.1	Food consumption (g/day per kg ^{0.67}) during the experimental period of REM sleep deprivation and nicotine treatment.	136
Figure 3.1.1(a)	Food consumption (g/day per kg ^{0.67}) during the Morris Water Maze test.	137
Figure 3.1.2	Body weight (g) gain during 72 hours of adaptation period.	139
Figure 3.1.2(a)	Body weight gain (g) during experimental period (72 hours REM sleep deprivation experiment and nicotine injection).	140
Figure 3.1.2(b)	Body weight gain (g) during the 6 day duration of the Morris Water Maze test.	141
Figure 3.2	Serum cotinine concentration.	143
Figure 3.3.1	The mean escape latency time for the first five days of the Morris Water Maze test.	145
Figure 3.3.1(a)	The mean escape latency time for the first five days of the Morris Water Maze test.	146
Figure 3.3.1(b)	Comparison of the escape latency time between the trial days for each of the six experimental groups.	147
Figure 3.3.2	The mean of distance travel for five days by rats exposed to the Morris Water Maze test.	149
Figure 3.3.2(a)	The mean of travelled distance for five days by rats	

	exposed to the Morris Water Maze test.	150
Figure 3.3.2(b)	Comparison of the distance travelled between the trial days for each of the six experimental groups.	151
Figure 3.4	The mean of swimming speed for five days during the Morris Water Maze test.	153
Figure 3.4.1	The mean of swimming speed for five days during the Morris Water Maze test.	154
Figure 3.4.2	Comparison of the swimming speed between the trial days for each of the six experimental groups.	155
Figure 3.5	The mean of time spent in zone 1 (zone in which platform was located) on the sixth day (Probe test) by Morris Water Maze test.	157
Figure 3.5.1	Trajectory swimming pattern for all six groups of rats on day 6 of the Morris water mazeWater Maze test.	158
Figure 3.6	Positive immunohistological expression of the DREAM (A and a), BDNF (B and b) and phosphorylated CREB (Ser133) (C and c).	160
Figure 3.6(a)	Dark staining of the nucleus was completely absent when omitting primary antibody (DREAM) (A), secondary antibody (B), ABC (C) and DAB (D).	161
Figure 3.6.1	Distribution of DPN expression on the rat's hippocampus at 4× objective lens magnification.	164
Figure 3.6.1(a)	Distribution of DPN in the cornus ammonis 1 (CA1)	

	of rats hippocampus at 10× objective lens magnification.	165
Figure 3.6.1(b)	Distribution of DPN in the cornus ammonis 2 (CA2) of rats hippocampus at 10× objective lens magnification.	166
Figure 3.6.1(c)	Distribution of DPN in the cornus ammonis 3 (CA3) of rats hippocampus at 10× objective lens magnification.	167
Figure 3.6.1(d)	Distribution of DPN in the Dentate Gyrus (DG) of rats hippocampus at 10× objective lens magnification.	168
Figure 3.6.1(e)	Comparison of DPN in the hippocampal CA1 (A), CA2 (B), CA3 (C) and DG (D) regions between the groups.	169
Figure 3.6.2	Distribution of pCPN expression on the rat's hippocampus at 4× objective lens magnification.	173
Figure 3.6.2(a)	Distribution of pCPN in the cornus ammonis 1 (CA1) of rats hippocampus at 10× objective lens magnification.	174
Figure 3.6.2(b)	Distribution of pCPN in the cornus ammonis 2 (CA2) of rats hippocampus at 10× objective lens magnification.	175
Figure 3.6.2(c)	Distribution of pCPN in the cornus ammonis 3 (CA3)	

	of rats hippocampus at 10× objective lens magnification.	176
Figure 3.6.2(d)	Distribution of pCPN in the Dentate Gyrus (DG) of rats hippocampus at 10× objective lens magnification.	177
Figure 3.6.2(e)	Comparison of pCPN in the hippocampal CA1 (A), CA2 (B), CA3 (C) and DG (D) regions between the groups.	178
Figure 3.6.3	Distribution of BPN expression on the rat's hippocampus at 4× objective lens magnification.	182
Figure 3.6.3(a)	Distribution of BPN in the cornus ammonis 1 (CA1) of rats hippocampus at 10× objective lens magnification.	183
Figure 3.6.3(b)	Distribution of BPN in the cornus ammonis 2 (CA2) of rats hippocampus at 10× objective lens magnification.	184
Figure 3.6.3(c)	Distribution of BPN in the cornus ammonis 3 (CA3) of rats hippocampus at 10× objective lens magnification.	185
Figure 3.6.3(d)	Distribution of BPN in the Dentate Gyrus (DG) of rats hippocampus at 10× objective lens magnification.	186
Figure 3.6.3(e)	Comparison of BPN in the hippocampal CA1 (A),	

	CA2 (B), CA3 (C) and DG (D) regions between the groups.	187
Figure 3.7.1	Quantification analysis of the integrated density value. Columns represent the mean relative DREAM protein level.	189
Figure 3.7.2	Quantification analysis of the integrated density value. Columns represent the mean relative total CREB protein level.	191
Figure 3.7.2(a)	Quantification analysis of the integrated density value. Columns represent the mean relative ratio phospho/total CREB protein level.	192
Figure 3.7.3	Quantification analysis of the integrated density value. Columns represent the mean relative BDNF protein level.	194
Figure 3.8.1	Ultrastructural changes in the CA1 hippocampal neuron of the C group (A) and CN group (B).	197
Figure 3.8.1(a)	Ultrastructural changes in the CA1 hippocampal neuron of the R group (A) and RN group (B).	198
Figure 3.8.1(b)	Ultrastructural changes in the CA1 hippocampal neuron of the W group (A) and WN group (B).	199
Figure 3.8.1(c)	Mean scores for changes in the cytoplasm (A), nucleus (B), mitochondria (C), RER (D) and GA (E) of the hippocampal CA1 neurons between the	

	groups.	200
Figure 3.8.2	Ultrastructural changes in the CA2 hippocampal neuron of the C group (A) and CN group (B).	203
Figure 3.8.2(a)	Ultrastructural changes in the CA2 hippocampal neuron of the R group (A) and RN group (B).	204
Figure 3.8.2(b)	Ultrastructural changes in the CA2 hippocampal neuron of the W group (A) and WN group (B).	205
Figure 3.8.2(c)	Mean scores for changes in the cytoplasm (A), nucleus (B), mitochondria (C), RER (D) and GA (E) of the hippocampal CA2 neurons between the groups.	206
Figure 3.8.3	Ultrastructural changes in the CA3 hippocampal neuron of the C group (A) and CN group (B).	209
Figure 3.8.3(a)	Ultrastructural changes in the CA3 hippocampal neuron of the R group (A) and RN group (B).	210
Figure 3.8.3(b)	Ultrastructural changes in the CA3 hippocampal neuron of the W group (A) and WN group (B).	211
Figure 3.8.3(c)	Mean scores for changes in the cytoplasm (A), nucleus (B), mitochondria (C), RER (D) and GA (E) of the hippocampal CA3 neurons between the groups.	212
Figure 3.8.4	Ultrastructural changes in the DG hippocampal neuron of the C group (A) and CN group (B).	215

Figure 3.8.4(a)	Ultrastructural changes in the DG hippocampal neuron of the R group (A) and RN group (B).	216
Figure 3.8.4(b)	Ultrastructural changes in the DG hippocampal neuron of the W group (A) and WN group (B).	217
Figure 3.8.4(c)	Mean scores for changes in the cytoplasm (A), nucleus (B), mitochondria (C), RER (D) and GA (E) of the hippocampal DG neurons between the groups.	218
Figure 5.1	Summary of changes in protein level and expression of DREAM, pCREB and BDNF; and ultrastructure scores during REMsd and acute nicotine treatment.	266

LIST OF APPENDICES

- | | |
|------------|--------------------------------------|
| Appendix 1 | Animal ethics approval |
| Appendix 2 | Sample size calculation |
| Appendix 3 | List of materials used in this study |
| Appendix 4 | Preparation of solutions and buffers |
| Appendix 5 | Result report for rat cotinine ELISA |

LIST OF ABBREVIATIONS

5-HT	: serotonin
ABC	: avidin-biotinyl complex
AKT	: anti-apoptotic kinase
AMP	: adenosine monophosphate
AMPA	: α -amino-3-hydroxy-5-methyl-4-isoxazolepropionic acid
ANOVA	: analysis of variance
APS	: ammonium persulphate
ARASC	: Animal research and service centre
ATP	: adenosine triphosphate
ARAS	: ascending reticular activating system
ACh	: acetylcholine
AChE	: acetylcholinesterase
BC	: before Christ
BCA	: bicinehoninic acid
BDMA	: benzyl dimethylamine
BDNF	: brain-derived neurotrophic factor
BF	: basal forebrain
BPN	: BDNF positive neuron
BSA	: bovine serum albumin
BW _g	: body weight gain
C	: control group

Ca ²⁺	: calcium
CA	: connus ammonis
CA1	: connus ammonis region 1
CA2	: connus ammonis region 2
CA3	: connus ammonis region 3
CaM	: calmodulin
cAMP	: cyclic adenosine monophosphate
cDNA	: complementary DNA
CMN	: cellular-molecular-network
CN	: control and nicotine treated group
CNS	: central nervous system
CBP	: CREB binding protein
CPEB	: cytoplasmic polyadenylation element binding protein
CRE	: cAMP-responsive element
CREB	: cyclic AMP response element binding protein
DAB	: diaminobenzidine
DB	: diagonal band
DDSA	: dodecyl succinic anhydride
DG	: dentate gyrus
dH ₂ O	: deionised water
DNA	: deoxyribonucleic acid
DOW	: disk over water
DPN	: DREAM positive neuron

DRE	: downstream response element
DREAM	: downstream regulatory element antagonist modulator
DT	: distance travelled
EC	: entorhinal cortex
ECL	: enhanced chemiluminescent
EEG	: electroencephalogram
EF1	: first EF hand
EF2	: second EF hand
EF3	: third EF hand
EF4	: fourth EF hand
EL	: escape latency
ELISA	: enzyme linked immunosorbent assay
EMG	: electromyogram
EOG	: electrooculogram
ER	: endoplasmic reticulum
ETC	: electron transport chain
Fc	: food consumption
GA	: Golgi apparatus
GABA	: gamma-aminobutyric acid
GC	: granule cell
Glu	: glutamate
H ₂ O ₂	: hydrogen peroxide
HCl	: hydrochloric acid

HI	: hypoxic-ischemic
IDV	: integrated density values
IgG	: immunoglobulin G
IHC	: immunohistochemistry
HRP	: horseradish peroxidase
i.p	: intraperitoneal
K ⁺	: potassium
KChIPs	: voltage-gated potassium(Kv) channels-interacting proteins
Kv	: voltage-gated potassium
LC	: locus coeruleus
LDT	: laterodorsal tegmentum
LTD	: long term depression
LTP	: long term potentiation
MAPK	: mitogen- activated protein kinase
Mg ²⁺	: magnesium
MNA	: methylnadic anhydride
mPRF	: medial pontine reticular formation
mRNA	: messenger RNA
MS	: medial septum
MWM	: Morris water maze
n	: number
NA	: noradrenaline

Na ²⁺	: sodium
nAChR	: nicotinic acetylcholine receptor
NaCl	: sodium chloride
Na ₂ HPO ₄	: disodium hydrogen phosphate
Na ₂ HPO ₄ .7H ₂ O	: sodium phosphate heptahydrate
NaH ₂ PO ₄ .H ₂ O	: sodium dihydrogen phosphate dehydrate
NaHCO ₃	: sodium bicarbonate
NaOH	: sodium hydroxide
NGF	: nerve growth factor
NGS	: normal goat serum
NMDA	: N-methyl-D-aspartate
NPY	: neuropeptide Y
NREM	: non-rapid eye movement
NT	: neurotrophin
OD	: optical density
PAGE	: polyacrylamide gel electrophoresis
PB	: phosphate buffer
PBS	: phosphate buffered saline
pCREB	: phosphorylated cyclic AMP response element binding protein
pCPN	: pCREB positive neuron
PFA	: paraformaldehyde
PI3	: phospho inositol 3 phosphates

P13K	: phosphoinositide 3-kinase
PKA	: protein kinase A
PKC	: protein kinase C
POMC	: pro-opiomelanocortin
PPT	: pedunculopontine tegmentum
PT	: probe test
PS	: paradoxical sleep
R	: rapid eye movement group
REM	: rapid eye movement
REMSd	: REM sleep deprivation
RER	: rough endoplasmic reticulum
RIPA	: radioimmune precipitation
RN	: rapid eye movement and nicotine treated group
RNA	: ribonucleic acid
RNc	: raphe nucleus
ROS	: reactive oxygen species
rpm	: revolutions per minutes
SDS	: sodium dodecyl sulphate
SDS-PAGE	: sodium dodecyl sulphate polyacrylamide gel
S.E.M	: standard error mean
Ser	: serine
SNc	: substantia nigra compacta
SPSS	: statistical package of social sciences software

SS	: swimming speed
SWS	: slow wave sleep
TBS	: tris buffer saline
TBS-T20	: tris buffer saline-Tween 20
TBS-TX	: tris buffer saline- Triton X-100
TEM	: transmission electron microscopy
TEMED	: N,N,N'N'-tetramethyldiamine
TGN	: trans-Golgi network
TMB	: tetramethylbenzidine
tPA	: tissue plasminogen activator
TrkB	: tyrosine kinase B
UCP1	: uncoupling protein 1
UPR	: unfolded protein response
VTA	: ventral tegmental area
W	: wide platform group
WN	: wide platform and nicotine treated group

**PERUBAHAN STRUKTUR, EKSPRESI PROTEIN DREAM, BDNF DAN CREB
DI DALAM HIPOKAMPUS; DAN PEMBELAJARAN RUANGAN DAN
MEMORI TERHADAP TIKUS YANG MENGALAMI KEKURANGAN TIDUR
PERGERAKAN MATA CEPAT (REM) SELEPAS RAWATAN NIKOTIN AKUT**

ABSTRAK

Kekurangan tidur fasa ‘pergerakan mata cepat’ (REMsd) telah terbukti mengganggu tahap pembelajaran ruangan dan keupayaan memori, manakala rawatan nikotin akut berupaya mengelakkan kesan tersebut. Kajian ini dijalankan untuk menyiasat mekanisme REMsd dan penggunaan nikotin dalam menghalang gangguan pembelajaran ruangan dan memori dengan menyiasat ekspresi ‘*downstream regulatory element antagonist modulator*’ (DREAM), ‘*cyclic AMP response element binding protein*’ (CREB), dan ‘*brain-derived neurotrophic factor*’ (BDNF); dan perubahan ultraselular sel-sel hipokampus tikus REMsd. Tikus Sprague Dawley jantan yang berusia 10 minggu dan mempunyai berat sekitar 200-250 g telah dibahagikan kepada enam kumpulan. Kumpulan pertama (Kawalan (C), n=24) dan kedua (Kawalan dan nikotin (CN), n=24) terdiri daripada tikus kawalan yang bebas bergerak; kumpulan 3 (REMsd (R), n=24) dan 4 (REMsd dan nikotin (RN), n=24) terdiri daripada tikus dengan REMsd yang diaruh menggunakan teknik pasu tertangcup selama 72 jam; kumpulan kelima (Platform lebar (W), n=24) dan keenam (Platform lebar dan nikotin (WN), n=24) terdiri daripada tikus yang terdedah kepada persekitaran eksperimen yang sama seperti tikus REMsd, tetapi pasu tertangcup untuk kumpulan ini adalah lebih lebar, dan membolehkan tikus tidur. Kumpulan C, R, dan W disuntik secara subkutaneus dengan salin manakala kumpulan CN, RN dan WN disuntik dengan 1 mg/kg nikotin

secara subkutaneus setiap 12-jam sekali selama 72 jam. Kaedah ‘*Morris Water Maze*’ (n=36), digunakan untuk menentukan pembelajaran ruangan dan memori, dimana 5 hari pertama adalah ujian ‘*escape latency*’, manakala pada hari terakhir ujian ‘*probe*’. Pengambilan makanan dan berat badan setiap kumpulan tikus diukur semasa tempoh penyesuaian, tempoh induksi 72 jam dan semasa tempoh ujian MWM. Bagi setiap kumpulan, hippocampi telah dikeluarkan untuk imunohistokimia (IHC) (n=36), pemblotan Western (WB) (n=36), dan analisis mikroskop transmisi elektron (TEM) (n=36) secara berasingan. REMsd dalam kumpulan R dan RN disahkan melalui hiperfagia dan kehilangan berat badan. Dalam tikus kumpulan R, gangguan pembelajaran ruangan dan memori dapat di kesan; analisis TEM menunjukkan kerosakan dalam sitoplasma, nukleus, mitokondria, retikulum endoplasma kasar (RER) dan alat golgi (GA); IHC memperlihatkan bahawa tikus-tikus ini mempunyai jumlah neuron positif DREAM yang lebih banyak, tetapi bilangan neuron-neuron pCREB dan BDNF yang lebih sedikit pada kawasan hippocampal iaitu ‘*cornu ammonis*’ (CA) - CA1, CA2 CA3, dan ‘*dentate gyrus*’ (DG); dan keputusan ini konsisten dengan analisis WB. Tikus-tikus dari kumpulan RN yang dirawat nikotin menunjukkan kesan REMsd yang berkurangan. Kesimpulannya, kajian ini menunjukkan bahawa rawatan nikotin akut terhadap REMsd boleh mengurangkan gangguan pembelajaran dan memori ruang dengan (1) mengurangkan kerosakan ultrastruktur hippocampus, (2) mengurangkan ekspresi dan aras protein DREAM, dan (3) meningkatkan ekspresi dan aras protein pCREB dan BDNF, dalam hippocampi tikus REMsd.

**STRUCTURAL CHANGES, EXPRESSION OF DREAM, BDNF AND CREB
PROTEINS IN THE HIPPOCAMPUS; AND SPATIAL LEARNING AND
MEMORY OF RAPID EYE MOVEMENT (REM) SLEEP-DEPRIVED RATS
UPON ACUTE NICOTINE TREATMENT**

ABSTRACT

Rapid eye movement sleep deprivation (REMsd) has been shown to disturb spatial learning and memory performance, while acute nicotine treatment prevented these effects. This study was conducted to investigate the mechanisms of REMsd and the use of nicotine in preventing impairments in spatial learning and memory by investigating the expression of '*downstream regulatory element antagonist modulator*' (DREAM), '*cyclic AMP response element binding protein*' (CREB), and '*brain-derived neurotrophic factor*' (BDNF) proteins; and ultracellular changes in the rat's hippocampal cells. Ten-week-old male Sprague Dawley rats weighing 200-250 g were divided into six groups. The first (Control (C), n=24) and second to eliminate nicotine effect on control group (Control and nicotine (CN), n=24) groups comprised freely-moving control rats; groups 3 (REMsd (R), n=24) and 4 (REMsd and nicotine (RN), n=24) consisted of rats with REMsd induced using the inverted flower pot technique for 72 hours; and the fifth (Wide platform (W), n=24) and sixth (Wide platform and nicotine (WN), n=24) groups comprised rats which were exposed to the same experimental environment as the REM sleep-deprived rats, however, the inverted flower pot used for this group was wider, hence enabling the rats to sleep. The C, R, and W groups were injected with normal saline subcutaneously while the CN, RN and WN groups were injected with 1 mg/kg nicotine subcutaneously every 12-hourly for 72

hours. The Morris Water Maze (MWM) (n=36) instrument was used to determine the spatial learning and memory performances, by which the initial 5 days was for the 'escape latency' test and the final day 'probe' test. Food consumption and body weight gain were measured for all groups during adaptation, 72 hours induction period, and during MWM period. For each group, hippocampi were removed for immunohistochemistry (IHC) (n=36), Western blotting (WB) (n=36), and transmission electron microscopy (TEM) analysis (n=36) separately. The REMsd in the R and RN groups was confirmed by REMsd-induced hyperphagia and weight loss. In the rats of R group, there was marked spatial and memory impairment; TEM analysis showed damages in the cytoplasm, nuclei, mitochondria, rough endoplasmic reticulum (RER) and golgi apparatus (GA); IHC showed that these rats had higher total number of DREAM-positive neurons, but lower total number of pCREB- and BDNF-positive neurons in the 'cornu ammonis' (CA) - CA1, CA2 CA3, and 'dentate gyrus' (DG) hippocampal regions; and these results were consistent with those of the WB analysis. Nicotine-treated group RN rats, showed reduction of REMsd effects. In conclusion, this study showed that acute nicotine treatment in REMsd reduced impairments in spatial learning and memory by (1) attenuating the hippocampal ultrastructure damage, (2) reducing the DREAM protein expression and level, and (3) increasing the pCREB and BDNF protein expressions and levels, in the hippocampi of REMsd rats.

CHAPTER 1

INTRODUCTION

1.1 SLEEP

Sleep is one of the physiological needs in human and most of the living organisms. While sleeping, one will become senseless to the surroundings and is unable to remember any activities occurred during this phase. Thus, it is regarded as a resting state in which the body becomes inactive, the muscles relaxed, the eyes closed and the mind is unconscious (Datta and MacLean, 2007). This observation eventually yields to the conclusion that sleep is a passive state of the whole body and mind. It is a time for rest and recovery from the stresses of everyday life.

In contrast to the perception, previous studies revealed that sleep is indeed an active condition. Apart from energy restoration, sleep enhances the process of biosynthesis as well as cellular and subcellular membrane repair (Mackiewicz *et al.*, 2007; Maret *et al.*, 2007; Vyazovskiy and Harris, 2013; Ribeiro-Silva *et al.*, 2016). It also provides protection against oxidative stress (Silva *et al.*, 2004; Periasamy *et al.*, 2015), modulates gene expression (Guzman-Marin *et al.*, 2006; Grønli *et al.*, 2014), increases the brain protein synthesis (Nakanishi, 1997; Grønli *et al.*, 2014) which in turn promotes neurogenesis (Guzman-Marin *et al.*, 2007; Guzman-Marin *et al.*, 2008). As a result, sleep contributes significantly to the process of learning and memory (through memory encoding and consolidation) and brain plasticity (Samkoff and Jacques, 1991;

Peigneux *et al.*, 2001; McDermott *et al.*, 2003; Walker and Stickgold, 2006; Walker, 2008).

1.1.1 History of sleep study

The phenomenon of sleep has been contemplated by the philosophers since the Vedic civilisation, from 16th to 11th century B.C. (Datta *et al.*, 2005; Datta and MacLean, 2007). However, scientific studies of sleep began with the discoveries of electroencephalogram (EEG) (Datta and MacLean, 2007). Datta and MacLean (2007) reviewed that in the mid 30's, Loomis and his colleagues showed the differences between waking, sleep and dreaming EEG patterns on human subjects. They also reviewed a work by Klaue in 1937 using cats as subjects. According to Datta and MacLean (2007), Klaue had discovered that EEG showed two different patterns during sleep. The first pattern was slow cortical waves occurred during light sleep, followed by speed up waves at the time of deep sleep (Klaue, 1937; Datta and MacLean, 2007).

In 1953, Aserinsky and Kleitman conducted several series of sleep experiments involving normal adult subjects, and recorded the movement of the eye (using electrooculogram (EOG)), gross body, EEG, as well as heart and respiratory rates during sleep. They found out that 3 hours after sleep begins, the eyes rapidly moved, EEG pattern together with the pulse and respiratory rate increased, lasted on the average of 20 minutes (Aserinsky and Kleitman, 1953). This cluster reoccurred around 2 hours (on average) after the first appearance (Aserinsky and Kleitman, 1953), and discovered it

was related to dream (Aserinsky and Kleitman, 1953; Dement and Kleitman, 1957), in which Dement and Kleitman (1957) called it rapid eye movement (REM) sleep.

To get a clear definition of REM sleep, a study using sleeping cats a year later has been established, which led to two different cortical EEG patterns called ‘sleep pattern’ (slow rhythms with higher voltage, and some spindle patterns waves) and ‘activated sleep pattern or REM sleep’ (fast rhythms with low voltage waves) (Dement *et al.*, 1958). It was in this study, Dement and his teams initially used water tank technique to deprive the sleep of the studied cats, and evaluate EEG patterns in sleep deprived cats. Several other researchers also noticed two different patterns of sleep which were said to be slow wave sleep (SWS), later known as non-rapid eye movement sleep (NREM); and paradoxical sleep (PS), which is known as REM sleep (Suchecki *et al.*, 2000; Datta and MacLean, 2007) (Figure 1.1). As the name implies, PS sleep (NREM sleep) indicates that during this sleep stage, the brain gets activated, however, this condition is contrary with muscle tone, in which muscle become weak or known as atonia (Suchecki *et al.*, 2000; Datta and MacLean, 2007).

1.1.2 Sleep process

Before sleep is initiated, our body is in the state of wakefulness. While awake, we are aware of our surroundings and muscles are active. Previous studies utilised polysomnography to study this phase (Aston-Jones and Bloom, 1981; Aeschbach *et al.*, 2008; Seibt *et al.*, 2012). Thus, it is essential to discuss the waking state and waking-

promoting system in order to understand the generation of sleep as well as types of sleep.

Waking and sleep stages can be distinguished using three associated cardinal physiological parameters, namely brain wave activities, eye movements, and muscle tone. Therefore, each of this state can be studied using polysomnogram, which consists of the combination of EEG (brain activities), EMG (muscle tone) and EOG (eye movements) (Datta and MacLean, 2007).

1.1.2(a) Waking state

Waking state can be divided into two stages, which are active and quiet waking (Aston-Jones and Bloom, 1981). Active waking stage is described by the exploratory and alert state in which EEG showed a high frequency but a low amplitude and non-periodic signal. Meanwhile, EMG portrays a high amplitude tonic activity with frequent phasic bursts (Aston-Jones and Bloom, 1981). The EMG in quiet waking state displays similar pattern with the active state but lesser phasic burst, while EEG demonstrates the lack of spindle activity with about twice the amplitude as well as more periodic signals (Hobson, 2005) (Figure 1.1).

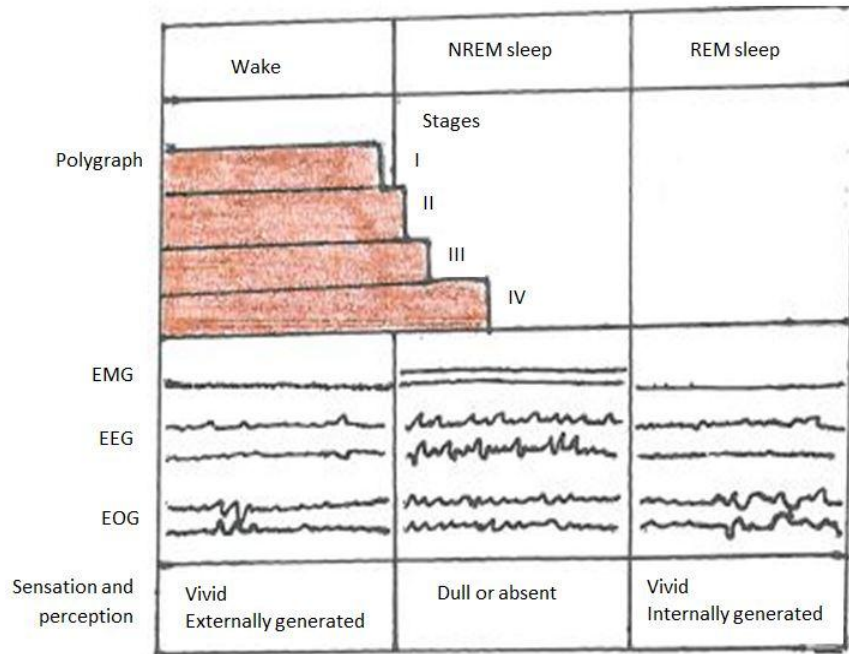


Figure 1.1: Waking and sleep stages. Adapted from Hobson (2005).

1.1.2(b) Wake-promoting system

In 1916, a Viennese neurologist, Von Economo began to observe his patients that slept excessively and this condition is known as encephalitis lethargica (Saper *et al.*, 2005; Schwartz and Roth, 2008). He was the first that reported the ascending arousal system that kept the forebrain awake and this system originates in the brainstem (Saper *et al.*, 2005). Thirty years later, Moruzzi and Magoun studied the same system and introduced it as the wake-promoting system, by which activation of this system is responsible for the alertness of an organism and prevents it from falling asleep (Jones, 2005; Datta and MacLean, 2007; Schwartz and Roth, 2008).

Some groups of neurons that make up the wake-promoting systems are located within the ascending reticular activating system (ARAS) (situated within the rostral of pons through midbrain reticular formation) and secrete their own types of neurotransmitter (Jones, 2005b; Saper *et al.*, 2005; Datta and MacLean, 2007). These wake-promoting groups of cells are: noradrenergic cells in the locus coeruleus (LC), serotonergic cells in the raphe nuclei (RNc), cholinergic cells in the pedunculopontine tegmentum (PPT), glutamatergic cells in the midbrain, and dopaminergic cells in the substantia nigra compacta (SNc) and ventral tegmental area (VTA) (Figure 1.2).

1.1.2(c) Sleep initiation

Initiation of sleep in human is a complex passive process and this happens during stage 1 of sleep by which the waking stage is shifted to the NREM phase (Datta and

MacLean, 2007; Datta, 2010) (Figure 1.1). The most preferred theory in understanding this event is reticular deactivation theory. This theory posits that the reduction of ascending impulses from the reticular formation that maintains the brain activity during wakefulness is responsible for sleep (Datta and MacLean, 2007; Datta, 2010). Therefore, the phase of sleep initiation occurs when the ascending impulses activity is decreasing.

In 2007, after gathering more information about physiological changes of sleep initiation, Datta and his colleague, MacLean, came out with the theory of “activity-dependent metabolites homeostatic” to explain the transition period of wakefulness to sleep. The sleep initiating metabolic factors that are important in metabolites homeostasis are neuroinhibitory amino acids, gamma-aminobutyric acid (GABA), glycine, adenosine, prostaglandin D2 (PGD2) and cytokines such as interleukin-I beta (IL-1 β) and tumour necrosis factor alpha (TNF α) (Datta, 2010). According to this theory, metabolic factors are increasing while awake, but the clearance rate is lower, thus they accumulate inside the body and brain (Datta, 2010). When these metabolites reach the certain threshold, they need to be reduced to the basal level (Datta and MacLean, 2007; Datta, 2010). This is to ensure that the homeostasis of metabolites will take place by clearing the accumulated metabolites and reducing the metabolites production rates (Datta and MacLean, 2007; Datta, 2010). Thus, the body and brain react by lowering the activity of the wake-promoting neuronal system. As a result, sleep is initiated (Datta and MacLean, 2007; Datta, 2010).

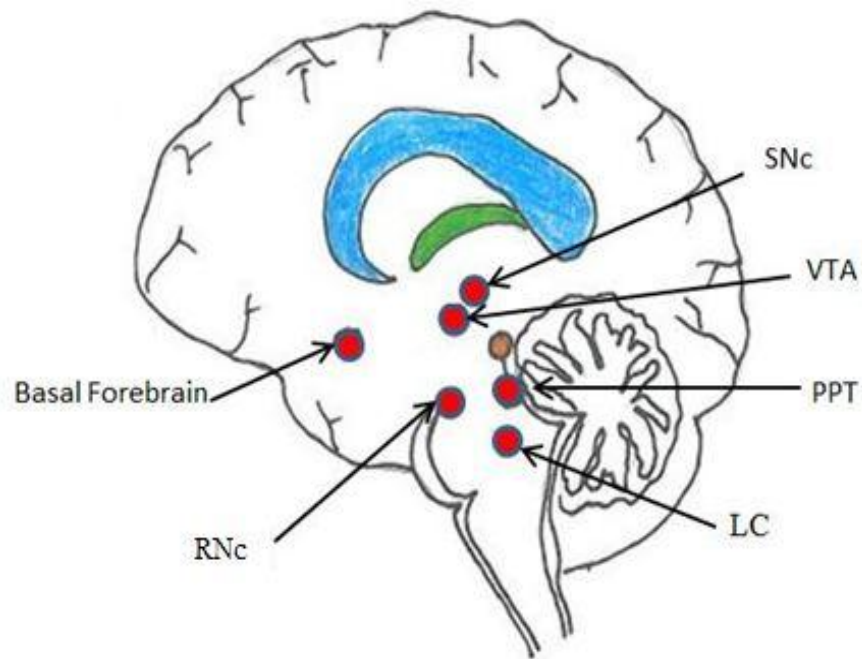


Figure 1.2: A schematic drawing showing key components of the ascending arousal system. The groups of neurons that are responsible to the wake-promoting system located in LC (locus coeruleus), RNC (raphe nuclei), PPT (pedunculopontine tegmentum), SNc (substantia nigra compacta) and VTA (ventral tegmental area). Adapted from Saper *et al.* (2005).

1.1.3 Sleep categories

From the scientific perspective, sleep is described as a physiological process occurring as a result of the reduction of receptivity toward the exterior stimuli which coexists with a loss of consciousness (Rasch and Born, 2013). Sleep has been categorized into two phases known as the non-rapid eye movement (NREM) and rapid eye movement (REM) (Smith, 1995; Maquet, 2001; Hobson, 2005). The full cycle between NREM and REM in human is around 90 minutes while in rodents is approximately 10 minutes (Trachsel *et al.*, 1991; Benington *et al.*, 1994; Prince and Abel, 2013).

1.1.3(a) NREM sleep phase

NREM sleep phase occurs after the initiation of sleep, controlled by the activity of waking promoting systems in which the neuronal activity in thalamocortical networks depends on the metabolites level in the brain. Therefore, both the wake-promoting system and brain metabolites level are responsible for controlling the incoming sensory signals from the thalamus to the cerebral cortex.

Thalamo-cortical relay neurons (neurons that relay sensory information to the cortex) and thalamic reticular neurons (prevent thalamocortical relay neurons from transferring sensory information to the cortex when activated), are two types of neurons in the thalamus that are responsible for NREM sleep phase (Steriade *et al.*, 1993; Steriade and Timofeev, 2003; Datta, 2010). In generating NREM sleep, the increment of

waking promoting system and metabolites, GABA_B during wakefulness should be reduced (Datta and MacLean, 2007; Datta, 2010). Increasing of metabolites, such as GABA_B, causes the excitation of thalamic reticular cells. When thalamic reticular cells are activated, they will inhibit the thalamocortical relay neurons and block the transmission of sensory impulses to the cortex, which leads to the generation of NREM sleep phase (Datta, 2010).

The different stages of NREM sleep phase can be identified using cortical EEG recordings. There are four stages of NREM sleep phase in human, namely stage I, II, III and IV (Maquet, 2001; Hobson, 2005; Pizza *et al.*, 2011) as shown in Figure 1.1. Stage I shows the transition of wakefulness and NREM sleep phase (Pizza *et al.*, 2011). Then, stage II takes place and is characterised by the presence of K complex (a negative sharp wave followed by slower positive component) and slow oscillation with peculiar sleep spindles (Pizza *et al.*, 2011). Finally, stage III and IV, which are characterised by the presence of low-frequency wave activity which indicates the deepest sleep of NREM and termed as Slow Wave Sleep (SWS) (Maquet, 2001; Pizza *et al.*, 2011). In animals such as cat, rats and mouse, there are only two stages of NREM sleep phase known as stage SWS I and SWS II (Datta and MacLean, 2007).

1.1.3(b) REM sleep phase

REM sleep phase generation is relatively more complex than NREM sleep phase. During the REM sleep, cortical EEG shows relatively fast rhythm and low amplitude, while eye ball rapidly moves and muscle tone becomes weak. This phenomenon is

known as paradoxical sleep (PS) (Maquet, 2001; O'Malley and Datta, 2013). It is also referred to as highly activated brain in a paralysed body (Maquet, 2001; O'Malley and Datta, 2013). There are also other signs of REM sleep such as fluctuations in core body temperature and cardio-respiratory rhythms (Datta and MacLean, 2007). Furthermore, invasive EEG in non-human primates (Tamura *et al.*, 2013) and rats (Colgin, 2016) shows slow activity (theta) rhythm in the hippocampus as well as P-waves, a spiky field potentials in the pons, lateral geniculate nucleus, and occipital cortex, which leads to the occurrence of vivid dreaming (Hutchison and Rathore, 2015).

These signs of REM sleep will occur when groups of neurons called REM-promoting neurons are activated and reach the certain threshold (Datta, 2010). The neurotransmitter that is essential in producing the set of REM signs is cholinergic neurotransmitter acetylcholine (ACh) that acts by exciting the populations of brainstem reticular formation neurons (Hobson, 2009; Ranjan *et al.*, 2010). There are other neuronal populations called REM-off neurons. These neurons release aminergic neurotransmitter serotonin (5-HT) or noradrenaline (NA) (Hobson, 2009; Ranjan *et al.*, 2010).

The physiological mechanism of REM sleep execution has been explained by cellular-molecular-network (CMN) model (Datta and MacLean, 2007; Datta, 2010). REM sleep starts from the activation of REM-promoting neurons, which are located in the pons and midbrain (Datta and MacLean, 2007; Datta, 2010). It then propagates to the basal forebrain (Ballinger *et al.*, 2016). According to the CMN model, REM sleep is

not regulated from a single centre, but is composed of several groups of distinct cells that are widely distributed as a network (Datta and MacLean, 2007; Datta, 2010).

In generating the REM sleep signs, these groups of network cells are initially excited by the increased level of ACh neurotransmitter, released from the cholinergic neurons in the pedunclopontine tegmentum (PPT) and laterodorsal tegmentum (LDT). The medial pontine reticular formation (mPRF) is then activated and consequently lead to the reduction or absent level of NA neurotransmitter (from the noradrenergic neurons in the locus coeruleus (LC)) and 5-HT neurotransmitter (from the aminergic neurons in the raphe nucleus (RNc)) (Datta and MacLean, 2007; Datta, 2010).

Activation of mPRF will then trigger activation of the cholinergic neurons in the basal forebrain (BF) which sends its projection to the hippocampus, neocortex, and amygdala (Woolf, 1991; Baghdoyan *et al.*, 1993; Ballinger *et al.*, 2016). Therefore, the interaction of REM-on and REM-off network cells as well as the oscillating changes between the above neurotransmitters that eventually generates the REM sleep signs (Figure 1.3).

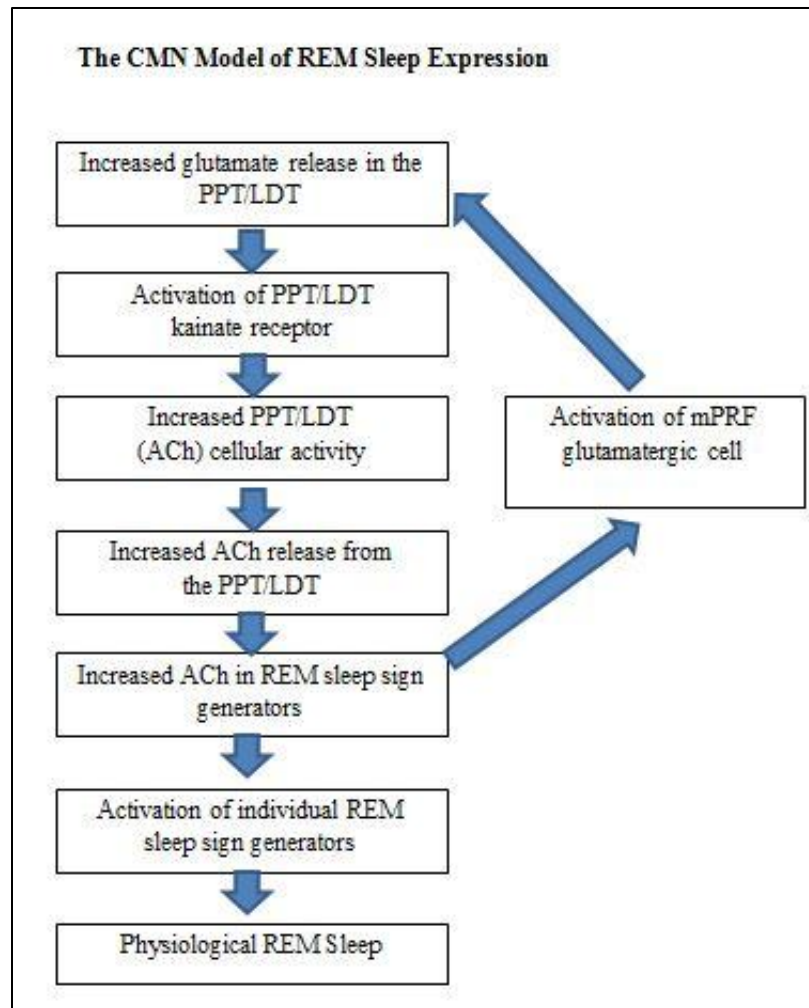


Figure 1.3: The expression of REM sleep using Cellular-Molecular-Network (CMN) model on the activity of cholinergic and aminergic system. Adapted from Datta and MacLean (2007).

PPT - pedunclopontine tegmentum

LDT - laterodorsal tegmentum

ACh - acetylcholine

mPRF - medial pontine reticular formation

REM - rapid eye movement

1.1.3 (c) Mechanism of REM sleep generation

Initiation of sleep begins in the area rich of cholinergic neurons known as PPT and LDT. At first, kainate receptors on the cholinergic neurons are activated by the release of glutamate (Datta and Siwek, 2002; Datta and MacLean, 2007). This triggers the release of ACh from cholinergic cells (Datta and Siwek, 2002; Datta and MacLean, 2007). The ACh activates each of the groups that generate REM sleep signs and REM sleep-inducing site in the mPRF. During activation of cholinergic cells in PPT and LDT, the noradrenergic neurons in the LC and serotonergic neurons in the RNc are inhibited by GABAergic cells located in those particular areas (Datta and MacLean, 2007; Datta, 2010). Therefore, the release of aminergic neurotransmitter is reduced, and this modulation initiates the REM sleep signs (Datta and MacLean, 2007; Datta, 2010).

1.1.3 (d) REM sleep maintenance

The episodes of REM sleep maintenance depend on the ratio between cholinergic and aminergic neurotransmitters within the cell groups (Datta and Siwek, 2002; Datta and MacLean, 2007; O'Malley and Datta, 2013). During wakefulness and NREM sleep, the REM sleep sign-generator remains in the turned-off condition by which the ratio of aminergic and cholinergic neurotransmitter is 1:1 (Datta, 2010; O'Malley and Datta, 2013). In this case, the activity of aminergic and cholinergic neurons is proportionate and the activity of both types of neurons show approximately the same level of activity during wakefulness. It is also noted that during NREM sleep the activities of both types

of neurons are equally reduced (Datta and MacLean, 2007; Datta, 2010; O'Malley and Datta, 2013).

However, at the time of REM sleep, the ratio of aminergic to cholinergic activity is 0:0.6, which indicates the inhibition of the aminergic activity while the activity of cholinergic neurons is comparatively high and more active than in wake (Datta and Siwek, 2002; Datta and MacLean, 2007; Datta 2010; O'Malley and Datta, 2013). This results in a brain state that is largely deficient in aminergic modulation and dominated by acetylcholine (Walker and Stickgold, 2004).

The activity of cholinergic cells in PPT and LDT is maintained by the continuous activation of glutamate that is released from the ACh-induced mPRF activity (Datta and MacLean, 2007; Datta, 2010). The glutamate also activates the aminergic and GABAergic cells in the LC and RNC; however, the inhibition of LC and RNC precedes the activation of aminergic cells due to the local release of GABA in the LC and RNC (Datta and MacLean, 2007; Datta, 2010). In addition to that, the activation of mPRF also stimulates the BF cholinergic neurons, in which hippocampus receives the majority of the cholinergic input from the BF via two nuclei, the medial septal (MS) and diagonal band (DB) (Woolf, 1991; Ballinger *et al.*, 2016).

1.2 REM SLEEP DEPRIVATION

Sleep is vital for the good health, well-being and support of life. An animal model has been accepted as a potentially useful strategy in order to understand the functions

and the regulation of REM sleep as well as its deprivation (Pedrazzoli *et al.*, 2009; Orzeł-Gryglewska, 2010; Colavito *et al.*, 2013; Toth and Bhargava, 2013).

1.2.1 REM sleep deprivation (REMSd) models

The model for REMsd can be developed in animals using a simple technique known as classic platform method, which is either a single-platform or multiple-platform method (Medeiros *et al.*, 1998; Suchecki *et al.*, 1998; Machado *et al.*, 2004; Machado *et al.*, 1998; Mueller *et al.*, 2008; Alkadhi *et al.*, 2013).

In 1964, the single inverted flower pot method was developed by Jouvett and his co-worker to elicit the sleep loss in cats. Then a year later, Cohen and Dement adapted this method to rats (Suchecki *et al.*, 1998; Machado *et al.*, 2004; Tufik *et al.*, 2009). Using this model, there is a confined tank filled with water, that surrounds a single platform usually 6.5 cm in diameter, in which a rat is placed on top of it. The surrounding water is at a specified level such that the rat will be slipped into the water when it undergoes loss of muscle tone (atonia) induced by REM sleep. The animal awakens when in contact with water and this scenario prevents the occurrence of REM sleep (Suchecki *et al.*, 1998; Machado *et al.*, 2004; Tufik *et al.*, 2009). This method leads to the REMsd-related morbidities (Koban and Swinson, 2005; Koban *et al.*, 2008) while the occurrence of NREM sleep loss is minimum (Machado *et al.*, 2006; Mueller *et al.*, 2008).

Previous studies have shown that the plasma adrenocorticotrophic hormone (ACTH) and plasma corticosterone increased in animals exposed to the single platform

technique due to stress induced by social isolation (Suchecki *et al.*, 1998; Suchecki and Tufik, 2000). Other studies observed aggressive behaviour (Kushida *et al.*, 1989; Martins *et al.*, 2008; Orzel-Gryglewska, 2010). In addition, some studies have shown that, immobilisation from the single flower pot deprived both REM and NREM sleep (Suchecki and Tufik, 2000; Pawlyk *et al.*, 2008).

Even though the single platform method has been used to produce REMsd, factors such as isolation stress, muscle fatigue due to movement restriction and wetness have become the confounding variables (Suchecki *et al.*, 1998; Machado *et al.*, 2004; Machado *et al.*, 2006). Thus, in 1981, Van Hulzen and Coenen introduced multiple platform paradigms in which a rat is placed inside a larger water tank that contains several platforms, which enable the rat to ambulate and reduce the movement restriction (Gulyani *et al.*, 2000; Machado *et al.*, 2004). The multiple platform paradigm does exclude immobilization stress; however, stress due to social isolation cannot be eliminated (Suchecki *et al.*, 2000; Suchecki and Tufik 2000; Machado *et al.*, 2004; Machado *et al.*, 2006). Using this method, the weight of adrenal gland was shown to increase and there was a reduction in the thymus weight due to stress (Coenen and Van Luutelaar, 1985). Thus, a modified multiple platform method is carried out in order to minimise the social isolation induced stress (Suchecki *et al.*, 2000; Suchecki and Tufik, 2000; Machado *et al.*, 2004; Machado *et al.*, 2006).

The modified multiple platform model aiming to suppress REM sleep simultaneously in a group of rats involves many small platforms for a group of rats (Suchecki *et al.*, 2000; Suchecki and Tufik, 2000; Machado *et al.*, 2004; Machado *et al.*,

2006). However, this method results in more stress and lower occurrences of sleep episodes as compared to the previous single platform method (Medeiros *et al.*, 1998; Machado *et al.*, 2004). Even though this technique reduces the social isolation and locomotor restrictions, but the forced awakening secondary to social interactions results in stress with an associated increase of plasma corticosterone and ACTH levels (Suchecki *et al.*, 1998; Suchecki and Tufik, 2000). Moreover, a study using large multiple platform revealed an elevation of ACTH levels of the rats though it was not as high as in rats that are exposed to the small multiple platforms (Suchecki *et al.*, 1998). Hence, the social interactions in the water tank generate stress among study rats (Medeiros *et al.*, 1998; Machado *et al.*, 2004).

Later, a method known as disk-over-water (DOW) is used to study chronic sleep deprivation (Landis *et al.*, 1992; Rechtschaffen and Bergmann, 1995; Rechtschaffen *et al.*, 1999; Lader *et al.*, 2006). According to this paradigm, an experimental rat is placed on one side of a separated horizontal disk that is hanged over a shallow tray of 2 to 3 cm deep water (Landis *et al.*, 1992; Rechtschaffen and Bergmann, 1995; Rechtschaffen *et al.*, 1999; Lader *et al.*, 2006). The disk was automatically rotated at low speed when the rat is starting to sleep and keep the rat awake, thus in order to avoid falling into the water, the rat was forced to walk in an opposite direction of the rotating disk (Rechtschaffen and Bergmann, 1995). During this procedure, sleep states were continuously monitored from the theta activity, EMG and EEG (Landis *et al.*, 1992; Rechtschaffen and Bergmann, 1995; Rechtschaffen *et al.*, 1999; Lader *et al.*, 2006). This method has been shown to selectively deprive REM sleep by 86% (Landis *et al.*, 1992;

Rechtschaffen and Bergmann, 1995) and can be as high as 99% (Kushida *et al.*, 1989; Rechtschaffen and Bergmann, 1995).

The different methods of sleep deprivation are not only to provide a model of sleep deprivation, but it is also to reduce (or eliminate) the other stress factor that may be developed during the deprivation process. This is because stress can be a confounding factor for the REMsd, thus it may generate comorbidities.

1.2.2 Effect of REMsd on the animal behaviour

Exposing REMsd to the animals may develop several effects that have been studied previously. REM sleep deprived rats fail to groom, this leads to progressive debilitation manifested in scrawny appearance with dishevelled, clumped and yellowing fur (Kushida *et al.*, 1989; Rechtschaffen *et al.*, 1989; Rechtschaffen and Bergmann, 1995; Gulyani *et al.*, 2000; Hossein *et al.*, 2000). Other physical appearances that can be seen are aggressive behaviour (Medeiros *et al.*, 1998; Suchecki and Tufik, 2000; Orzeł-Gryglewska, 2010), weight loss and hyperphagia (Kushida *et al.*, 1989; Rechtschaffen *et al.*, 1989; Youngblood *et al.*, 1997; Koban *et al.*, 2006; Martins *et al.*, 2008; Barf *et al.*, 2012).

In addition, REM sleep-deprived animals showed several internal body changes such as increase of plasma catecholamines, hypothyroidism, reduced core temperature, elevated metabolic rate and energy expenditure (Rechtschaffen *et al.*, 1989; Rechtschaffen and Bergmann, 1995; Koban *et al.*, 2006; Mueller *et al.*, 2008). Furthermore, hormonal studies have shown that anabolic hormones (Growth hormone

(GH), Insulin-like growth factor I (IGF-I), prolactin and leptin) are reduced in REM sleep-deprived animal (Everson and Crowley, 2004; Koban *et al.*, 2006).

Two most important characteristics of REMsd are hyperphagia that was contrarily associated with loss of body weight (Rechtschaffen and Bergmann, 1995; Youngblood *et al.*, 1997; Koban *et al.*, 2006; Martins *et al.*, 2008; Barf *et al.*, 2012). In accordance with hyperphagia after REMsd, the hormones for food intake within the hypothalamus and brainstem known as neuropeptide Y (NPY), pro- opiomelanocortin (POMC) and leptin have changed (Mathieu-Kia *et al.*, 2002; Koban and Swinson, 2005; Koban *et al.*, 2006; Koban *et al.*, 2008; Moraes *et al.*, 2014). These changes are due to the increase of the NYP gene expression within the hypothalamus while the POMC gene expression (the counterpart of NPY) decreased (Koban *et al.*, 2006; Koban *et al.*, 2008). In addition, after 5 days of REMsd, the secretion of a satiety hormone by white adipocytes, known as serum leptin (hormone that gives blunting appetite signal after binds to receptors within the hypothalamus and brainstem) decreased more than 50 percent in rats which demonstrated hyperphagia and loss of body weight (Koban and Swinson, 2005).

Studies have shown that REMsd increases resting metabolic rate, and thus reduces the body weight despite hyperphagia (Koban and Swinson, 2005; Koban *et al.*, 2008; Martins *et al.*, 2008). This hypermetabolic state is believed to be mediated via Uncoupling Protein 1 (UCP1), a 32 kDa inner mitochondria membrane protein that plays a major role in cellular respiration by allowing proton leakage, which resulted in

thermodynamic energy dissipating as heat in the cells of brown adipose tissue (Koban and Swinson, 2005; Koban *et al.*, 2006; Martins *et al.*, 2008; Christie *et al.*, 2011).

REMsd also leads to the increment of the energy expenditure by increasing the use of body fats and proteins but with a normal glucose uptake (Kushida *et al.*, 1989; Rechtschaffen and Bergmann, 1995). Several studies confirmed that excessive use of the body fat leads to negative energy balance state, which in turn reduce the body weight (Koban and Swinson, 2005; Venancio and Suchecki, 2015).

1.2.3 Effect of REMsd on the neuronal morphology

The effects of REMsd on the morphology of neurons were first observed by Pieron in 1921 (Majumdar and Mallick, 2005). After REM sleep deprived, neurons become shrunken (Majumdar and Mallick, 2005; Biswas *et al.*, 2006), nucleus showed an ectopic appearance of heterochromatin (Majumdar and Mallick, 2005), while nuclear volume decreased by 20-25% (Pedrazzoli *et al.*, 2009). Other changes are vacuolization of the protoplasm, fragmentation and the disappearance of nissl and neurofibrils (Majumdar and Mallick, 2005). These changes confirmed that neuronal morphology and structure are both affected by REMsd (Majumdar and Mallick, 2005). However, the size of the neurons in rat brain cells changes and the changes are dependent on the physiological function and neurotransmitter content of the neuronal cells. For example, the size of cholinergic neurons decreases, but serotonergic neurons increase after REMsd (Rajan *et al.*, 2010). Furthermore, in studying the occurrence of apoptosis in

REM sleep-deprived rats, Biswas and his co-worker (2006) discovered that it occurs after 6 days of REMsd.

1.2.4 Effect of REMsd on the learning and memory

There is a large body of evidence from previous studies showing a strong correlation between sleep deprivation and learning and memory impairment in both humans and animals (Polzella, 1975; Smith, 1995; Smith and Rose, 1996; McDermott *et al.*, 2003; Guan *et al.*, 2004; Ferrara *et al.*, 2008). REM sleep has an essential role in learning and memory formation in the hippocampus (Marshall and Born, 2007). Therefore, deprivation of REM sleep impairs hippocampus-dependent learning and memory (McDermott *et al.*, 2006; Tartar *et al.*, 2006; Alhaider *et al.*, 2010; Aleisa *et al.*, 2011). In addition to that, the activity of hippocampus has reduced after sleep loss (Yoo *et al.*, 2007), where EEG studies proved that sleep deprivation blocks long-term potentiation (LTP), in the hippocampal CA1 (McDermott *et al.*, 2003; Kim *et al.*, 2005; Tartar *et al.*, 2006; Alhaider *et al.*, 2010) and DG regions (Ishikawa *et al.*, 2006), but increased long term depression (LTD) (Tadavarty *et al.*, 2009) in the activity of neuron in CA1 and CA3 regions of the hippocampus.

1.3 LEARNING AND MEMORY

Learning and memory are fundamental higher brain functions which are closely related (Benfenati, 2013). According to the American Psychological Association, learning is the acquisition of knowledge or skill (Kazdin, 2000), whereas memory is the

process of retaining, reconstructing and expressing the acquired knowledge over time (Kandel *et al.*, 2014). Learning and memory cannot be directly measured, thus it can be analysed from the performance changes of an organism under particular conditions (Davis and Squire, 1984).

1.3.1 Learning in animal

In animal, learning can be detected from their behaviour. Learning behaviour in the animal can be classified as non-associated learning, associated learning and cognition learning. The non-associative learning in animal behaviour is the simplest learning condition which are habituation (an animal stops responding after repeated stimulus) and imprinting (learning that occurs at development stage of certain animal, in which the young animal imitates their parents' behaviour) (Squire, 1992b).

The associative learning is classified as the conditioning learning behaviour and operant conditioning. The conditioning learning behaviour can be further subdivided into conditional and unconditional stimulus (Squire, 1992b). According to Ivan Pavlov experiment using a dog, classical conditioning can be explained by a particular response (eg. dog is salivating) associated with one stimulus (eg. smell of food), and that stimulus is associated with a second stimulus (when the dog is trained with sound of bell accompanied with food, the dog will salivate, then with the sound of bell even without food, the dog will also salivate) (Squire, 1992b). Therefore, conditioning stimulus is the smell of food while unconditioning stimulus is the sound of bell ringing (Squire, 1992b).

Meanwhile, operant conditioning is when the reward or punishment will be given to animals after performing a behaviour (Squire, 1992b).

Finally, the cognition learning behaviour is a sophisticated learning behaviour such as problem solving and spatial learning. In problem solving, a German scientist, Wolfgang Kohler performed an experiment using chimpanzees. Kohler hung a banana in chimpanzee cage, but too high for them to reach. He then placed several boxes on the floor. The chimpanzees demonstrated cognitive learning when they solved the problem by stacking the boxes and climbing them to reach the banana (Runco, 1990; Gould, 2004).

There are varieties of paradigm to investigate spatial learning and the commonly used one is Morris water maze (MWM), which is introduced by Richard Morris. Using this method, an animal (usually rodents) is placed in a tank containing water and the animal learns how to swim to find and escape on a submerged platform guided by external cues (Morris, 1984). Using spatial information (animal's capacity to remember spatial cues), this animal learns how to locate a hidden underwater platform and escape into it. Therefore, this task is classified as learning with explicit associative memory that involves cognitive mapping (Morris, 1984; Smith, 1995; Rasch and Born, 2013; Kandel *et al.*, 2014). Thus in this study, we used MWM in developing rat's spatial learning and we focused on the explicit memory.